PHYSICAL REVIEW E **93**, 030601(R) (2016)

Reentrant network formation in patchy colloidal mixtures under gravity

Daniel de las Heras,* Lucas L. Treffenstädt, and Matthias Schmidt
Theoretische Physik II, Physikalisches Institut, Universität Bayreuth, D-95440 Bayreuth, Germany
(Received 7 December 2015; published 1 March 2016)

We study a two-dimensional binary mixture of patchy colloids in sedimentation-diffusion equilibrium using Monte Carlo simulation and Wertheim's theory. By tuning the buoyant masses of the colloids we can control the gravity-induced sequence of fluid stacks of differing density and percolation properties. We find complex stacking sequences with up to four layers and reentrant network formation, consistently in simulations and theoretically using only the bulk phase diagram as input. Our theory applies to general patchy colloidal mixtures and is relevant to understanding experiments under gravity.

DOI: 10.1103/PhysRevE.93.030601

Patchy colloids [1,2] are nano- to micron-sized particles with a solid core and a discrete number of interaction sites or patches. Pairs of patches can form reversible bonds which tie the particles together. By tuning the shape of the colloids, and the number and types of patches, one can find complex phase behavior and novel types of phases. Examples are empty liquids [3], network fluids with pinched phase behavior [4], lower critical points [5], and self-assembly into complex structures [6–8]. The bulk phase behavior of model patchy colloids has been investigated via computer simulations, using molecular dynamics and Monte Carlo (see, e.g., Refs. [3,9,10]). Wertheim's association theory [11] is a widely used approach since it accurately predicts [12–14] the structures observed in computer simulations. We hence have appropriate tools to analyze the bulk behavior of model patchy colloids. However, in a real experimental realization [15], it is often unavoidable that colloids are subject to gravity.

Gravitational and thermal energies are typically comparable in colloidal systems. Hence, gravity can have a strong effect and drive new complex phenomena, especially in mixtures, where colloidal particles can float on top of a fluid of lighter colloids [16], and very complex sequences of stacks can occur even for systems with rather generic bulk phase behavior [17–19]. Relating the bulk phase diagram to sedimentation-diffusion equilibrium is therefore of vital importance to adequately compare theoretical studies of bulk behavior to findings in sedimentation experiments [20].

In this Rapid Communication we study theoretically the bulk phase behavior of a two-dimensional mixture of patchy colloids, and use it to obtain the sedimentation behavior via a local density approximation [21]. We compare the results to extensive Monte Carlo simulations of the same mixture under gravity. Despite the simplicity of the bulk phase diagram of the model, we find very rich phenomenology under gravity, including reentrant network formation. Moreover, we show how to use the bulk phase diagram to systematically predict the sedimentation behavior.

Colloidal particles vary in size from nanometers to micrometers. Here, we model the colloids as a hard core (hard disk of diameter σ) with interaction sites or patches on the surface [see Fig. 1(a)]. The patches are disks of diameter $\delta = (\sqrt{5-2\sqrt{3}}-1)\sigma/2 \approx 0.12\sigma$ with their centers of mass equispaced on the surface of the particle. Two patches form a bond if they overlap, in which case the internal energy of the system decreases by $\epsilon = 1$. The chosen size of the patches ensures that only bonds involving two patches can be formed [22]. The two species differ in their number of patches and their buoyant masses. Species 1 (2) has three (two) patches, and we consider a range of ratios of the buoyant masses.

In Fig. 1(b) we show the bulk phase diagram in the plane of chemical potentials of the two species, μ_1 and μ_2, according to Wertheim's theory for scaled temperatures $k_BT/\epsilon = 0.10$ and 0.15, with k_B the Boltzmann constant. We use the implementation of the theory described in [23] with the bonding volume corresponding to our type of patches, $v_b = 4.4 \times 10^{-3}\sigma^2$. Previous studies [22,23] of this system have shown theoretical results to be in very good agreement with Monte Carlo simulation data. At the lower temperature there occurs a first-order phase transition between a high- and a low-density fluid phase. In the $\mu_1-\mu_2$ plane, the binodal, at which both fluid phases coexist, has a vertical asymptote ($\mu_2 \to -\infty$) that tends to the value of μ_1 at the phase transition of the monocomponent system with three patches (species 1). A pure system with only two patches can form only chains and does not undergo a phase transition due to the absence of branching. Hence, the binodal of the mixture ends at a critical point. We also plot the percolation line, which we have obtained with the generalization of Flory-Stockmayer (FS) percolation theory [24,25] to binary mixtures [26]. FS theory is based on the assumption that the particles form treelike clusters, i.e., closed loops are neglected, which is consistent with Wertheim's theory. The mixture percolates if the probability that a patch is bonded, f_b, is higher than a percolation threshold, p. For a mixture of bi- and trifunctional particles [26]

$$p = \frac{x+2}{4x+2}, \tag{1}$$

where $x = N_1/(N_1+N_2)$ is the molar fraction of species 1, with N_i the number of particles of species i. In the percolation region of the phase diagram [cf. Fig. 1(b)], a transient cluster spans the entire system volume. In the nonpercolated region the particles form clusters of only finite size. The percolation line intercepts the binodal on the gas side, very close to the critical point. Hence, the high-density phase is always percolated. We

*Corresponding author: delasheras.daniel@gmail.com

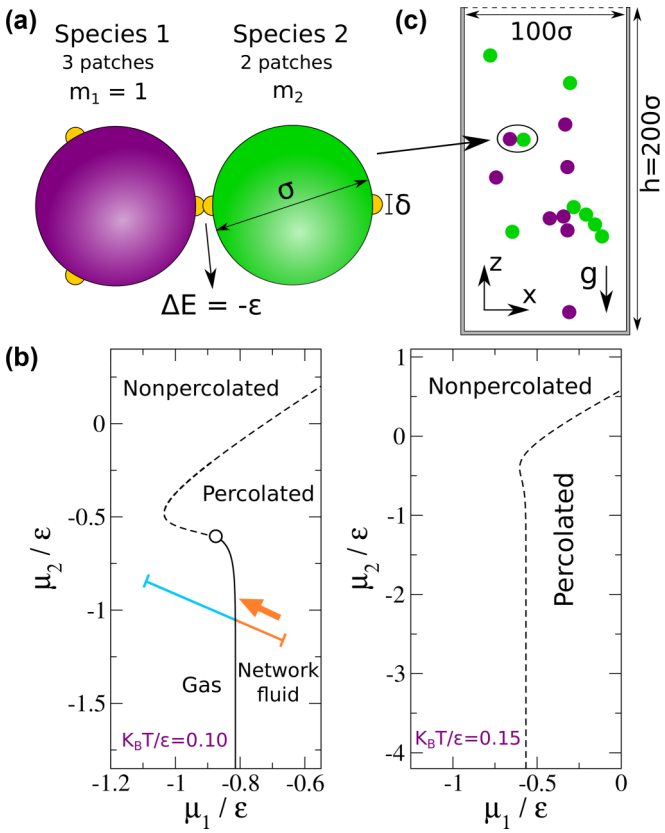

FIG. 1. (a) Illustration of the two types of patchy particles showing the inner hard core (diameter σ) and the patches (diameter δ). (b) Bulk phase diagram of the mixture at $k_BT/\epsilon = 0.10$ (left) and 0.15 (right) in the $\mu_1-\mu_2$ plane of chemical potentials according to Wertheim's theory. The black solid line is the binodal. The dashed line is the percolation line. The empty circle is the critical point. The binodal and the percolation line divide the phase diagram into percolated and nonpercolated regions as indicated. The straight line is an example of a sedimentation path. The arrow indicates the direction of the path from bottom to top. (c) Geometry of the simulation box to study sedimentation: a rectangular vessel (width 100σ and height $h = 200\sigma$) made of hard walls.

refer to this phase as a network fluid [26]. The second case, $k_BT/\epsilon = 0.15$, is above the upper critical temperature of the system. Hence the first-order gas-fluid transition is absent, but the percolation line divides the phase space into percolated and nonpercolated regions.

We study theoretically and with Monte Carlo simulations the mixture under gravity, i.e., in sedimentation-diffusion equilibrium. We simulate the system in the canonical ensemble, fixing the number of particles N_1 and N_2, the system volume V, and the temperature T. We confine the particles in a rectangular box of width 100σ and height $h = 200\sigma$ [see Fig. 1(c)]. The surface of the box consists of hard walls, i.e., the hard cores of the colloids cannot penetrate the walls. We apply an external gravitational field, $\phi_i(z) = m_i g z$, where g is the gravitational constant that we set to $g = 0.005\epsilon/(m_1\sigma)$, z is the vertical coordinate, and m_i is the buoyant mass of species i. We set $m_1 = 1$ as the unit of buoyant mass. To initialize the system we first run a simulation at a high temperature and take the last configuration as the initial state of the simulation at the temperature of interest. We run an equilibration stage until the energy fluctuates around a minimum value, and then perform 6×10^7 Monte Carlo steps to acquire the data. The data is averaged over three independent such simulations to improve statistics.

We compare the simulation results to theoretical predictions based on the concept of sedimentation paths [21,27] in the bulk phase diagram. We extend this theory to the case of systems exhibiting a percolation transition. We define a local chemical potential [21,27]:

$$\psi_i(z) = \mu_i^b - m_i g z, \quad i = 1,2, \tag{2}$$

with μ_i^b the bulk chemical potentials in absence of gravity. Combining Eq. (2) for $i = 1,2$ we obtain the sedimentation path:

$$\psi_2(\psi_1) = a + s\psi_1, \tag{3}$$

where a and s are constants given by

$$a = \mu_2^b - s\mu_1^b, \quad s = m_2/m_1. \tag{4}$$

In general, the gravitational length of the colloids, $\xi_i = k_BT/(m_i g)$, is much larger than any characteristic correlation length, which is typically of the order of the particles' sizes. Hence, we can assume that locally, i.e., at each value of z, the state of the system is well described by an equilibrium bulk state at the same chemical potential as the local chemical potential, i.e., $\psi_i(z) = \mu_i$ for both species $i = 1,2$. This local density approximation directly relates the sedimentation path, Eq (3), to the stacking sequence of the mixture. The sedimentation path is a straight line segment in the plane of chemical potentials μ_1 and μ_2. Each crossing between the sedimentation path and a boundary line between two phases corresponds to an interface in the sedimented sample. As an example, the path shown in Fig. 1(b) corresponds to a stacking sequence formed by a bottom network fluid and a top gas, because the path crosses the binodal line once.

The length of the path in the $\mu_1-\mu_2$ plane is proportional to the height of the container: $\Delta\mu_i = m_i g h$ with $\Delta\mu_i$ the difference in chemical potential between the top and the bottom of the sample. The buoyant masses fix the slope, Eq. (4), and the direction of the path, Eq. (2).

In order to compare to simulations, we calculate the average densities

$$\bar{\rho}_i = \frac{1}{h}\int_0^h dz\, \rho_i(z), \qquad i = 1,2 \tag{5}$$

with $\rho_i(z)$ the number density profile of species i which we obtain from the bulk equation of state $\rho_i(\mu_1,\mu_2)$ by calculating the local chemical potentials at a given height. Then, we move the path in the $\mu_1-\mu_2$ plane until the average densities equal those in the simulation, $\bar{\rho}_i = N_i/V$.

Figure 2 shows representative results for three different mixtures with different ratios of the buoyant masses. In all cases $N_1 = 4500$, $N_2 = 3000$, and hence $x = 0.6$. The scaled temperature is $k_BT/\epsilon = 0.15$, so the percolation line is the only feature present in the phase diagram.

First we analyze the case of equal masses $m_1 = m_2$ (first row in Fig. 2). The sedimentation path (a1) crosses the percolation line once, which generates the sequence percolated-nonpercolated (from bottom to top). Theoretical

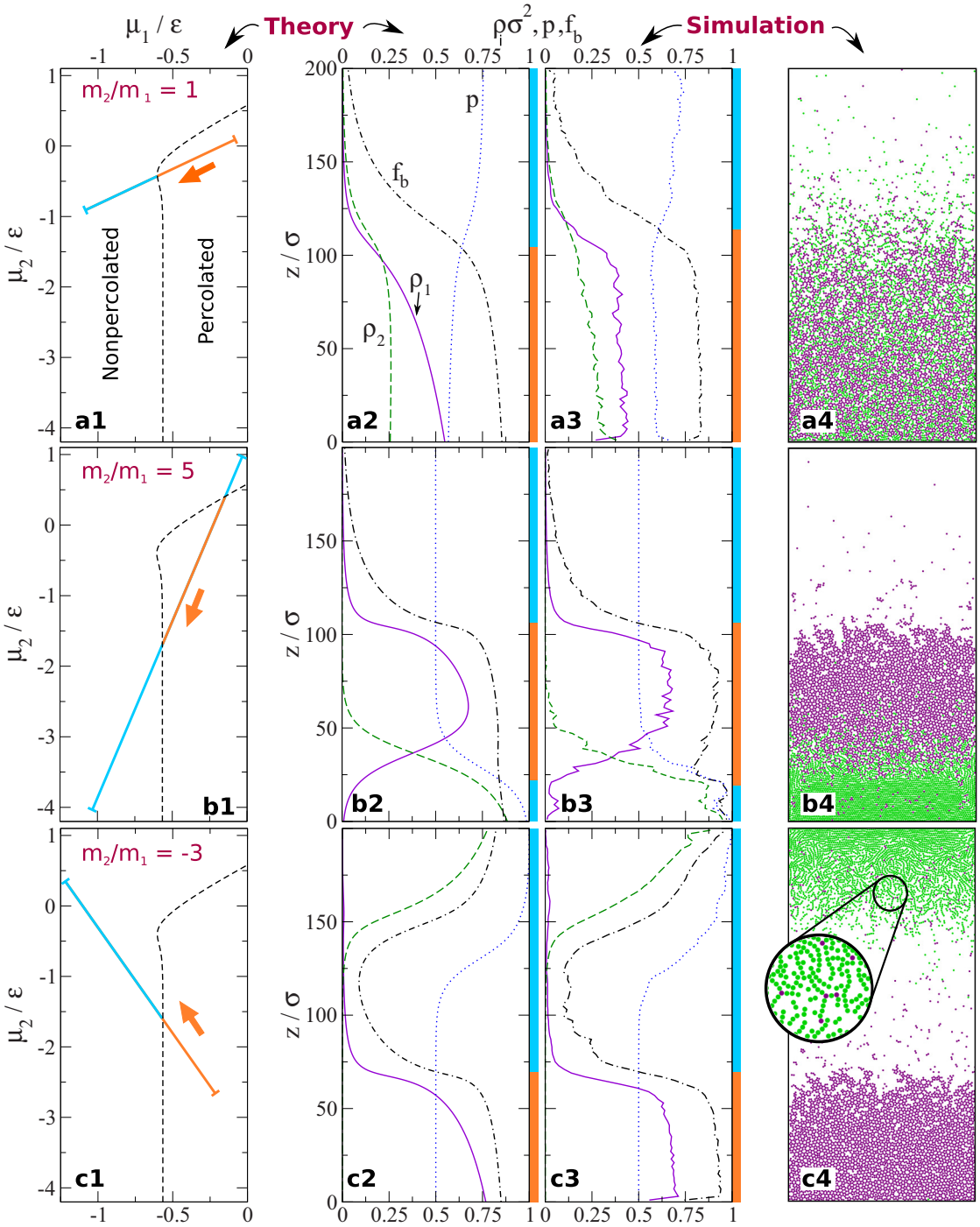

FIG. 2. Binary mixture of patchy colloids under gravity, $g = 0.005\epsilon/(m_1\sigma)$. First column: Phase diagram in the plane of chemical potentials $\mu_1 - \mu_2$ showing the sedimentation path (straight line). The arrows indicate the direction of the path from the bottom to the top of the sample. The path is colored in orange (cyan) in the percolated (nonpercolated) region. The height of the sample is $h = 200\sigma$. Second and third columns: Density profiles ρ_i of species $i = 1$ (solid violet line) and species $i = 2$ (dashed green line), percolation threshold p (dotted blue line), and probability that a patch is bonded f_b (dot-dashed black line). The orange (cyan) rectangle on the right of each panel indicates the percolated (nonpercolated) region, i.e., the region where $f_b > p$ ($f_b \leqslant p$). Results are according to theory (second column) and simulations (third column). The fourth column shows characteristic snapshots of the simulation. Each row corresponds to a different ratio of buoyant masses: $m_2/m_1 = 1$ (first row), $m_2/m_1 = 5$ (second row), and $m_2/m_1 = -3$ (third row). The inset in (c4) is a close view of a small region. In all cases the temperature is $k_B T/\epsilon = 0.15$, the composition of the mixture is $x = 0.6$, and in simulation $N = 7500$.

and simulation density profiles are shown in panels (a2) and (a3), respectively. We also show the bonding probability f_b and the percolation threshold p. Theory and simulation results for all quantities agree quantitatively. Both show the same stacking sequence and the interface between percolated and nonpercolated states, which occurs at $f_b = p$, is located at (almost) the same height. The percolated phase is a homogeneous mixture of both species, i.e., there is no demixing. A snapshot of the simulation is shown in (a4).

In the second row of Fig. 2 we increase the buoyant mass of bifunctional particles, $m_2 = 5m_1$. The sedimentation path in the plane of chemical potentials (b1) is substantially longer and steeper than in the previous example. This allows the path to cross the percolation line twice, generating a reentrant phenomenon. The path starts (bottom) in the nonpercolated region at high chemical potentials. The corresponding layer is a high-density nonpercolated phase, which is rich in bifunctional particles. Then, the path crosses the percolation line, giving rise to a percolated layer. Close to the bottom interface the percolated layer contains particles of both species. As the path enters the percolated region (increasing the height) the state changes to a network mainly composed of trifunctional particles. Finally, the path crosses the percolation line and a nonpercolated gas phase appears in the vessel. Again theory (b2) and simulation results (b3) are in very good agreement with each other. The snapshot (b4) illustrates the system.

The third row of Fig. 2 shows results for $m_2 = -3m_1$. Hence, the mass density of species 2 is smaller than the mass density of the solvent, and species 2 has a tendency to cream upwards. The path (c1), now with negative slope, crosses the percolation line once. The stacking sequence is bottom percolated and top nonpercolated, as in the case of equal masses (first row). However, in this case the bottom percolated stack is almost a pure system of trifunctional particles, and the top nonpercolated phase consists of two distinguishable regions. Close to the interface with the percolated region there is a gas phase and close to the top of the sample there is a dense layer primarily composed of bifunctional particles. Both theory and simulations show that this dense layer contains also a few particles with three patches [see inset in (c4)] but not in sufficient number to induce percolation.

Given the S shape of the percolation line, a straight sedimentation path can cross it three times, generating a reentrant phenomenon. This effect is very strong at low temperatures. In Fig. 3(a) we show the phase diagram at $k_B T/\epsilon = 0.1$, together with a sedimentation path for the case $m_2 = -5m_1$ and $g = 0.002\epsilon/(m_1\sigma)$. The path starts in the percolated region, then crosses the binodal entering the gas phase, and finally crosses twice the percolation line. The corresponding sequence consists of four layers: bottom percolated-nonpercolated-percolated-nonpercolated. This sequence constitutes a reentrant phenomenon for both percolated and nonpercolated phases. The bottom percolated-nonpercolated interface is very sharp since the path crosses the binodal line in the bulk phase diagram [see the density profiles in Fig. 3(b)]. The top nonpercolated-percolated interface is much wider. In this case, the path crosses the percolation line instead of the binodal. The upper percolated stack appears due to localized concentration of trifunctional particles, much heavier than the particles with two patches. Hence, the gravitational energy

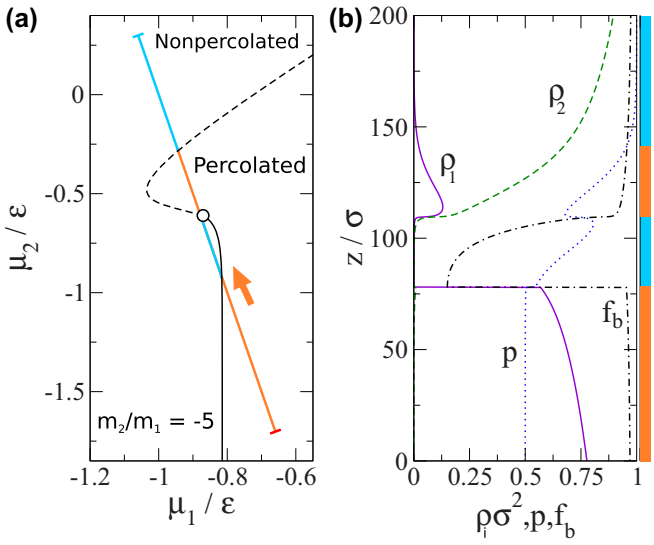

FIG. 3. (a) Bulk phase diagram according to Wertheim's theory in the plane of chemical potentials at $k_B T/\epsilon = 0.1$ together with a sedimentation path (straight line). The path corresponds to the case $g = 0.002\epsilon/(m_1\sigma)$, $m_2 = -5m_1$, $h = 200\sigma$ and average densities $\bar{\rho}_1\sigma^2 = 0.288$, $\bar{\rho}_2\sigma^2 = 0.313$. (b) Density profile ρ_i of species $i = 1$ (solid violet line) and species $i = 2$ (dashed green line), percolation threshold p (dotted blue line), and bonding probability f_b (dot-dashed black line) corresponding to the sedimentation path shown in (a). The orange (cyan) rectangle on the right of panel (b) indicates the percolated (nonpercolated) region, i.e., the region where $f_b > p$ ($f_b \leqslant p$). The sedimentation path (a) has the same color code.

would be lower if the heavier particles with three patches sedimented to the bottom stack. They are, however, far away from the bottom interface because they increase the bonding probability of particles with two patches, and hence decrease the free energy of bonding. Hence it is the balance between gravitational and bonding energies that drives the formation of this complex stacking sequence. Given the low temperature we have been unable to equilibrate the system with computer simulations. Advanced simulation techniques, such as "virtual-move" [28] or "aggregation-volume-bias" [29] Monte Carlo might alleviate the equilibration problem.

The bulk phase diagram of the two-dimensional mixture analyzed here and its corresponding three-dimensional mixture of bi- and trifunctional hard spheres [3,26] are qualitatively the same. Hence, we are confident that the sedimentation scenario is similar in three dimensions, since only the topology of the bulk phase diagram is relevant for determining the behavior under gravity.

Here we have used a strong gravitational field that affects the system at scales of a few particle lengths, as expected for micron-sized colloids [30]. In the case of nanoparticles, gravity affects the system at length scales of the order of 10^4–10^5 particle sizes. Our theory assumes the gravitational length to be much larger than any other correlation length, and hence it is expected to perform even better for such systems. Our theory might not be accurate in the vicinity of a critical point. However, we do not expect completely erroneous predictions, such as, e.g., a different stacking

sequence to occur. Nevertheless, the influence of gravity on critical phenomena is an important research topic (see, e.g., [31], which remains to be investigated for the case of patchy colloids).

Our results demonstrate that the presence of lateral walls, used in simulations and certainly present in experiments, does not have a negative impact on the development of complex stacking sequences.

Despite the simplicity of the bulk behavior of our system, displaying only a single binodal and one percolation line, the sedimentation behavior is quite complex. We therefore expect a much richer phenomenology when analyzing sedimentation of patchy colloids with complex bulk phase diagram, such as, e.g., those of patchy colloids with flexible bonds [32]. The ratio between buoyant masses is a key parameter that partially controls the stacking sequence. This ratio can be experimentally tuned by fabricating colloids with inner cores [33] made of different materials or by changing the density of the solvent.

The theoretical framework developed here is general and can be applied to study sedimentation of any patchy colloidal system using the bulk phase behavior as input. Here, we have used Wertheim's theory but other theories or even simulation techniques can be used to provide the bulk behavior. We have shown how structural crossover, such as the percolation line, in the bulk phase diagram relates to complex stacking sequences in sedimented systems. This extends our previous work [21,27], which was aimed only at phase coexistence. We have shown that the influence of gravity generates networks that are spatially inhomogeneous on the scale of the system size. This constitutes a further level of complexity of the self-assembly in patchy colloid systems. We have shown that the type of stacking can be precisely controlled by tuning simple material properties, such as the buoyancy masses of the particles. Our work paves the way for studying inhomogeneous patchy colloidal systems, where we expect a wealth of new phenomena occur, as is the case in the fields of inhomogeneous liquids and simple colloidal dispersions.

D.dlH. acknowledges support from the Portuguese Foundation for Science and Technology (FCT) through project EXCL/fis-nan/0083/2012.

D.dlH. and L.T. contributed equally to this work.

[1] E. Bianchi, R. Blaak, and C. N. Likos, Phys. Chem. Chem. Phys. **13**, 6397 (2011).
[2] Y. Wang, Y. Wang, D. R. Breed, V. N. Manoharan, L. Feng, A. D. Hollingsworth, M. Weck, and D. J. Pine, Nature (London) **491**, 51 (2012).
[3] E. Bianchi, J. Largo, P. Tartaglia, E. Zaccarelli, and F. Sciortino, Phys. Rev. Lett. **97**, 168301 (2006).
[4] J. Russo, J. M. Tavares, P. I. C. Teixeira, M. M. Telo da Gama, and F. Sciortino, Phys. Rev. Lett. **106**, 085703 (2011).
[5] L. Rovigatti, J. M. Tavares, and F. Sciortino, Phys. Rev. Lett. **111**, 168302 (2013).
[6] Q. Chen, S. C. Bae, and S. Granick, Nature (London) **469**, 381 (2011).
[7] G.-R. Yi, D. J. Pine, and S. Sacanna, J. Phys.: Condens. Matter **25**, 193101 (2013).
[8] D. J. Kraft, R. Ni, F. Smallenburg, M. Hermes, K. Yoon, D. A. Weitz, A. van Blaaderen, J. Groenewold, M. Dijkstra, and W. K. Kegel, Proc. Natl. Acad. Sci. USA **109**, 10787 (2012).
[9] Z. Zhang, A. S. Keys, T. Chen, and S. C. Glotzer, Langmuir **21**, 11547 (2005).
[10] C. De Michele, S. Gabrielli, P. Tartaglia, and F. Sciortino, J. Phys. Chem. B **110**, 8064 (2006).
[11] M. Wertheim, J. Stat. Phys. **42**, 459 (1986).
[12] J. Tavares, P. Teixeira, and M. T. da Gama, Mol. Phys. **107**, 453 (2009).
[13] B. D. Marshall, D. Ballal, and W. G. Chapman, J. Chem. Phys. **137**, 104909 (2012).
[14] F. Sciortino, E. Bianchi, J. F. Douglas, and P. Tartaglia, J. Chem. Phys. **126**, 194903 (2007).
[15] B. Ruzicka, E. Zaccarelli, L. Zulian, R. Angelini, M. Sztucki, A. Moussaïd, T. Narayanan, and F. Sciortino, Nat. Mater. **10**, 56 (2011).
[16] R. Piazza, S. Buzzaccaro, E. Secchi, and A. Parola, Soft Matter **8**, 7112 (2012).
[17] L. Luan, W. Li, S. Liu, and D. Sun, Langmuir **25**, 6349 (2009).
[18] H. H. Wensink and H. N. W. Lekkerkerker, Europhys. Lett. **66**, 125 (2004).
[19] D. de las Heras, N. Doshi, T. Cosgrove, J. Phipps, D. I. Gittins, J. S. van Duijneveldt, and M. Schmidt, Sci. Rep. **2**, 789 (2012).
[20] P. Woolston and J. S. van Duijneveldt, Langmuir **31**, 9290 (2015).
[21] D. de las Heras and M. Schmidt, Soft Matter **9**, 8636 (2013).
[22] J. Russo, P. Tartaglia, and F. Sciortino, Soft Matter **6**, 4229 (2010).
[23] L. Rovigatti, D. de las Heras, J. M. Tavares, M. M. Telo da Gama, and F. Sciortino, J. Chem. Phys. **138**, 164904 (2013).
[24] P. J. Flory, J. Am. Chem. Soc. **63**, 3083 (1941).
[25] W. H. Stockmayer, J. Chem. Phys. **11**, 45 (1943).
[26] D. de las Heras, J. M. Tavares, and M. M. Telo da Gama, Soft Matter **7**, 5615 (2011).
[27] D. de las Heras and M. Schmidt, J. Phys.: Condens. Matter **27**, 194115 (2015).
[28] S. Whitelam and P. L. Geissler, J. Chem. Phys. **127**, 154101 (2007).
[29] B. Chen and J. I. Siepmann, J. Phys. Chem. B **104**, 8725 (2000).
[30] C. P. Royall, J. Dzubiella, M. Schmidt, and A. van Blaaderen, Phys. Rev. Lett. **98**, 188304 (2007).
[31] E. A. G. Jamie, H. H. Wensink, and D. G. A. L. Aarts, Soft Matter **6**, 250 (2010).
[32] F. Smallenburg and F. Sciortino, Nat. Phys. **9**, 554 (2013).
[33] Y. Lu, Y. Yin, Z. Li, and Y. Xia, Nano Lett. **2**, 785 (2002).